Measurement of inner surface roughness of capillary by an x-ray reflectivity method*

Li Yu-De(李玉德)†, Lin Xiao-Yan(林晓燕), Tan Zhi-Yuan(谭植元), Sun Tian-Xi(孙天希), and Liu Zhi-Guo(刘志国)

The Key Laboratory of Beam Technology and Material Modification of Ministry of Education, College of Nuclear Science and Technology, Beijing Normal University, Beijing Radiation Center, Beijing 100875, *China*

(Received 31 December 2010; revised manuscript received 4 January 2011)

The inner surface roughness of a capillary is investigated by the reflectivity of x-rays penetrating through the capillary. The results are consistent with the data from atomic force microscope (AFM). The roughness measured by this new method can reach the order of angstroms with high quality capillaries.

Keywords: inner surface roughness, reflectivity method, capillary

PACS: 07.85.–m **DOI:** 10.1088/1674-1056/20/4/040702

1. Introduction

As a newly developed device for collimating or focusing x-rays, capillary x-ray optics has found more and more applications in many fields in recent years.[1−8] In order to obtain high-performance optics, the inner surface roughness of the capillaries becomes a key factor for the fabrication process. From the ray-tracing simulation, one can find that the capillary transmission efficiency will drop off seriously with a slight increase in the inner surface roughness. The accurate measurement and control of this important parameter is very important for the design and fabrication of capillary x-ray optics, and more efforts are being made to find methods to measure the inner surface roughness of capillaries so as to optimize fabrication processes. In 2005, Matsuura *et al.*[9] found that the roughness of their capillaries were in the range of 3 nm $\sim$ 6 nm in an area of 5 μm × 5 μm, and Mroczka *et al.*[10] observed a rough structure of 3.5 nm in height (1 μm × 1 μm) in a capillary fragment by using AFM. In 2008, Mroczka *et al.*[11] also used AFM to detect a capillary fragment with a large curvature and found that the results changed significantly while the area of measured region varied from 1 μm × 1 μm to 20 μm × 20 μm. With the AFM method, in order to measure the inner surface roughness, the capillary needs to be broken into pieces. Therefore, AFM is more suitable for plane sample measurement and cannot be used to detect the inner surface roughness of poly-capillary optics, which consists of a large number of capillaries. The diameters of these capillaries are often of the order of micrometers so they are too small to be probed by the AFM method.

The x-ray reflectivity technique is a commonly used non-destructive testing method to measure surface roughness.[12−14] However, it has not yet been used to investigate the inner surface roughness of capillaries. In the present paper, the experimental measurements of inner surface roughness of capillaries by the x-ray reflectivity method are reported.

2. Experiment

Measurements were performed with a θ–2θ type x-ray powder diffractometer and the x-ray radiation was produced by an x-ray tube with a copper anode of 50-μm diameter. A collimator of 50 μm was used to select the incidence beam size. A single column borosilicate glass capillary was placed on the sample stage. The main component of the borosilicate glass capillary was SiO_2. The length of the capillary was 40 mm, and the inner diameter was 1.08 mm. An Si detector was used to detect the reflected beam. Before the experiment, the collimator and the capillary were adjusted to be collinear and only half of the incident beam could directly transmit through the capillary,

*Project supported by the Natural Science Foundation of Beijing, China (Grant No. 1102019) and the Specialized Research Fund for the Doctoral Program of Higher Education of China (Grant No. 20100003120010).

†Corresponding author. E-mail: liyude@bnu.edu.cn

© 2011 Chinese Physical Society and IOP Publishing Ltd

as shown in Fig. 1(a). The sample stage was then rotated 180° around the point O, and there was still half of the incidence beam transmitting through the capillary. This ensured that the capillary was collinear with the incident beam. Then we rotated the sample stage around point O, part of the incidence beam was reflected by the inside surface of the capillary and part was directly transmitted through the capillary, as shown in Fig. 1(b). We located a 0.02-mm wide slit in front of the window of the detector, and then the detector could detect the direct beam and the reflected beam along a 2θ rotation.

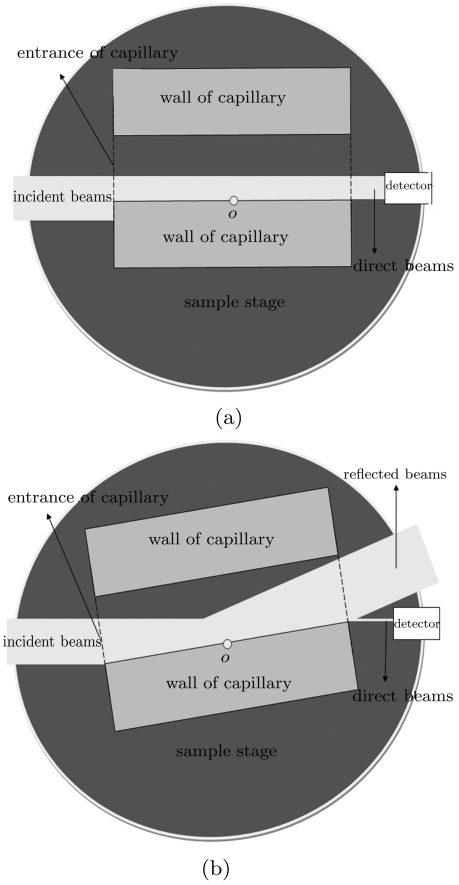


Fig. 1. Schematic diagram of the experiment.

Figure 2 shows the intensity distribution detected by the Si detector when the sample stage was rotated to 0.04° ($\theta = 0.04°$). The first peak comes from the direct beam and the second peak originates from the reflected beam. When $\theta = 0.08°$, the first peak disappeared, which means that all of the incident beams were reflected by the inner surface of the capillary. Then we started to measure the reflectivity of the inside surface of the capillary.

We first recorded the total intensity counts of the incident beam. Then the sample stage was rotated from 0.08° to 0.38°, and the reflected beam intensity was measured in steps of 0.01°. According to the definition of reflectivity $R_{\rm e}(\theta)$, we can obtain the reflectivity of the inner surface of the capillary at the incident angle θ,

$$R_{\rm e}(\theta) = \frac{I(\theta)}{I_0(\theta)}, \tag{1}$$

where $I_0(\theta)$ and $I(\theta)$ are respectively the incident intensity and the reflective intensity of x-rays at θ.

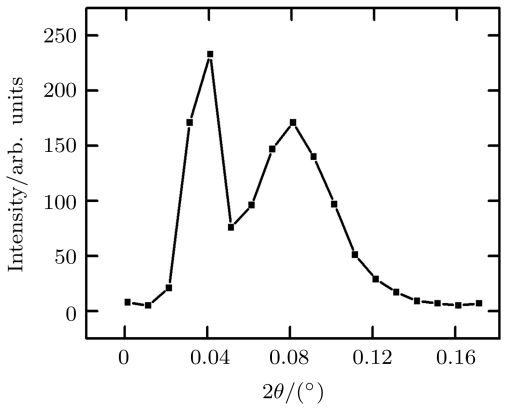


Fig. 2. Intensity distribution at $\theta = 0.04°$.

3. Results and discussion

It is well known that through the Fresnel formula, the reflectivity $R_{\rm t}(\theta)$ of x-rays on an ideal smooth surface can be expressed as

$$R_{\rm t}(\theta) = \frac{(a - \sin\theta)^2 + b^2}{(a + \sin\theta)^2 + b^2}, \tag{2}$$

where θ is the grazing angle, and a and b can be expressed as

$$a = \frac{1}{\sqrt{2}}\sqrt{\sqrt{(\sin^2\theta - \alpha)^2 + \gamma^2} + (\sin^2\theta - \alpha)},$$

$$b = \frac{1}{\sqrt{2}}\sqrt{\sqrt{(\sin^2\theta - \alpha)^2 + \gamma^2} - (\sin^2\theta - \alpha)},$$

where α determines the reflection and γ is related to the absorption of the x-rays on the surface.

Figure 3 shows a comparison between the experimental results and the theoretical results of the reflectivity. The points represent the reflectivities that we measured in the experiment, and the solid-line denotes the theoretical reflectivity of an ideal smooth surface, obtained from Eq. (2). Because of the surface roughness, we can see that all experimental results are smaller than the theoretical results.

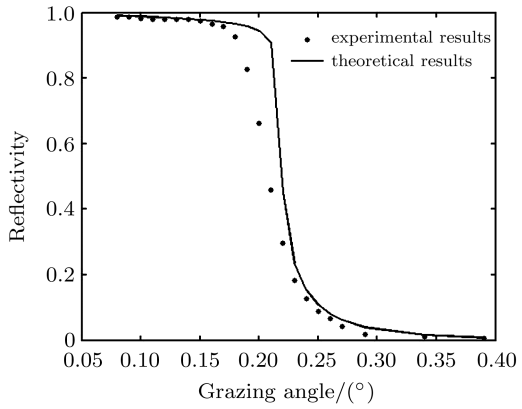


Fig. 3. Reflectivity versus grazing angle.

Taking the surface roughness into account, the reflectivity $R_{\rm e}(\theta)$ is usually written as

$$R_{\rm e}(\theta) = R_{\rm t}(\theta) \cdot \exp\left(-\frac{(4\pi\sigma\sin\theta)^2}{\lambda^2}\right), \tag{3}$$

where σ is a factor to count the effect of surface roughness, and λ is the wavelength of the incident x-rays.

According to Eq. (3), the surface roughness γ can be deduced as

$$\sigma = \frac{\lambda}{4\pi\sin\theta} \cdot \left(\ln\frac{R_{\rm t}(\theta)}{R_{\rm e}(\theta)}\right)^{1/2}. \tag{4}$$

In the experiment, the incident x-ray throughout the collimator has a divergence of 0.032°. So the incident intensity detected in the experiment is not the intensity of x-rays at a single incident angle θ, but the sum of the intensities at different incident angles in a range of $[\theta-\Delta\theta, \theta+\Delta\theta]$, where $\Delta\theta = 0.016°$ is the half divergence. The incident intensity measured in the experiment is expressed as I_0. Similarly, the reflected intensity is expressed as I. Thus the reflectivity $r_{\rm e}$ detected in the experiment should be

$$r_{\rm e} = \frac{I}{I_0} = \frac{\int_{\theta-\Delta\theta}^{\theta+\Delta\theta} I(\theta)\,{\rm d}\theta}{\int_{\theta-\Delta\theta}^{\theta+\Delta\theta} I_0(\theta)\,{\rm d}\theta}. \tag{5}$$

The intensities of incident x-rays at different incident angles should each be a constant due to the uniform distribution of the incident x-rays in the experiment, namely,

$$I_0(\theta) = c, \quad \theta \in (\theta-\Delta\theta, \theta+\Delta\theta), \tag{6}$$

where c is a constant.

According to Eqs. (1) and (6), $r_{\rm e}$ can be expressed as

$$r_{\rm e} = \frac{\int I_0(\theta)\cdot R_{\rm e}(\theta)\,{\rm d}\theta}{2\Delta\theta\cdot c}$$

$$= \frac{\int R_{\rm t}(\theta)\cdot\exp-\left(\dfrac{4\pi\sigma\sin\theta}{\lambda}\right)^2{\rm d}\theta}{2\Delta\theta}. \tag{7}$$

Using Taylor series expansion, we have

$$\exp-\left(\frac{4\pi\sigma\sin\theta}{\lambda}\right)^2 = 1 + \frac{-\left(\dfrac{4\pi\sigma\sin\theta}{\lambda}\right)^2}{1!} + \frac{\left(\dfrac{4\pi\sigma\sin\theta}{\lambda}\right)^4}{2!} + \cdots \tag{8}$$

As the second term is four orders of magnitude larger than the third term on the right-hand side of the above equation, the main contribution of $\exp-(4\pi\sigma\sin\theta/\lambda)^2$ comes from the first two terms, and the remaining terms can be neglected. Combining with the assumption of the first order approximation, equation (7) becomes

$$2\Delta\theta\cdot r_{\rm e} = \int R_{\rm t}(\theta)\cdot\left[1-\left(\frac{4\pi\sigma\sin\theta}{\lambda}\right)^2\right]{\rm d}\theta = \int R_{\rm t}(\theta)\,{\rm d}\theta - \left(\frac{4\pi\sigma}{\lambda}\right)^2\int R_{\rm t}(\theta)\cdot\sin^2\theta\,{\rm d}\theta. \tag{9}$$

So the roughness σ is

$$\sigma = \frac{\lambda}{4\pi}\sqrt{\frac{\int R_{\rm t}(\theta)\,{\rm d}\theta - 2\Delta\theta\cdot r_{\rm e}}{\int R_{\rm t}(\theta)\cdot\sin^2\theta\,{\rm d}\theta}}, \tag{10}$$

where $R_{\rm t}(\theta)$ is the theoretical result of the reflectivity of an ideal smooth surface, calculated by Eq. (2), and $r_{\rm e}$ is the experimental result of the reflectivity. The σ is calculated by Eq. (10). The experimental results are listed in Table 1. We can see that the inner surface roughness measured in the experiment is dependent on the incident angle θ. The main reason is that the measured area becomes smaller with the incident angles θ increasing. When incident angles $\theta = 0.17°$, the

Table 1. Theoretical and experimental reflectivities and surface roughnesses (1 Å = 0.1 nm).

$\theta/(°)$	$R_{\rm t}(\theta)$	$r_{\rm e}$	σ/Å
0.080	0.991	0.986	6.079
0.090	0.989	0.986	4.577
0.100	0.988	0.981	5.876
0.110	0.986	0.979	5.503
0.120	0.985	0.980	3.994
0.130	0.983	0.980	2.791
0.140	0.981	0.979	1.876
0.150	0.978	0.975	2.470
0.160	0.975	0.965	4.332
0.170	0.971	0.957	4.849

smallest measured area is about 1 mm^2. The results indicate that the roughness of the inner surface of a capillary is of the order of angstroms.

Figure 4 shows the AFM images of the outer surface of the capillary. Due to the large curvature and the small diameter of the capillary, an AFM image of the inner surface of the capillary is hard to obtain under ordinary experimental conditions. The

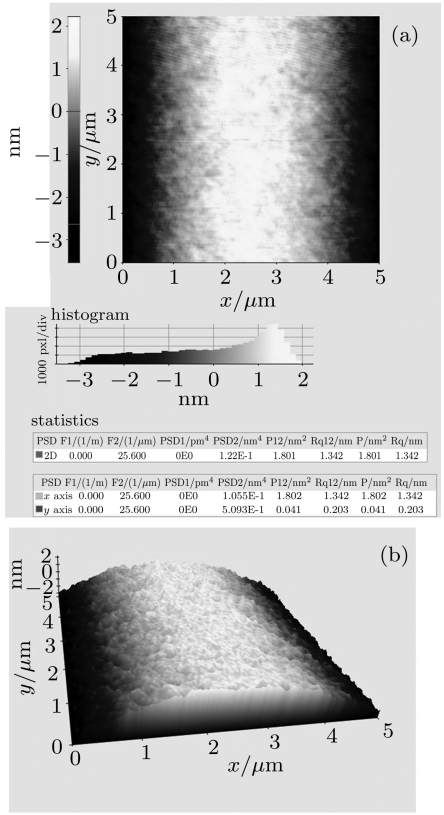


Fig. 4. AFM images of the outer surface of the capillary. (a) The 2D image of the same measured area (5 μm×5 μm). (b) The 3D image of the measured area (5 μm×5 μm).

roughnesses of the outer surface and the inner surface of a capillary are considered to be of the same order of magnitude, because they were fabricated by the same material and process. So it is convenient to take the outer surface roughness instead of the inner surface roughness for an order of magnitude estimate. As shown in Fig. 4(a), the two-dimensional (2D) roughness given by AFM is 1.342 nm (5 μm× 5μm). This is several times larger than our estimated result based on the reflectivity experiment. This is because the surface roughness given by AFM is the root-mean-square (RMS) height of the measured region. For a cylindrical surface, the 2D RMS value covers the contribution of the height difference along the x axis, as shown in Fig. 4(b). The height difference of the measured area along the x axis is several orders of magnitude larger than the real surface roughness, which makes the contribution of the real surface roughness neglected. As shown by the 3D image in Fig. 4(b), the RMS value along the x axis is 1.342 nm, and the RMS value along the y axis is 0.203 nm. For a larger area (10 μm×10 μm), the 2D roughness given by AFM becomes 5.165 nm, which equals the RMS value along the x axis, and the RMS value along the y axis is 0.253 nm. From these results, we can see that the RMS value along the y axis is consistent with the roughness given by the reflectivity method and it represents the real surface roughness of the capillary. These results also show that the 2D roughness given by AFM has a large difference between different measuring areas, which is because of the bending extent of the capillary.

4. Conclusion

From the experiments mentioned above, we can see that the 2D RMS value given by AFM with a capillary fragment is not the roughness of the inner surface and it is mainly influenced by the bending extent of the capillary. The RMS value along the axial direction of the capillary represents the real surface roughness of the capillary. Compared with this method, the reflectivity method is a kind of non-destructive measurement. Through the reflectivity method, we find that the inner surface roughness can reach the order of angstroms for the high-quality capillary. It is also convenient to use this method to detect the roughness of extremely small samples that cannot be detected by AFM, such as the small hollow fibres of a polycapillary. The roughness obtained from the reflectivity method is an average value of the roughness of a vast area (more than 1 mm^2). The results represent the characteristics of the whole capillary and may be very important for the design and fabrication of a total external reflection device in the future.

Acknowledgement

The authors thank Drs. Cai Wei and Li De-Wei (Beijing University of Aeronautics & Astronautics) for their help in the experiment.

References

[1] Lin X Y, Li Y D, Tan G T and Sun T X 2007 *Chin. Phys. Lett.* **24** 3368

[2] Bjeoumikhov A, Arkadiev V, Eggert F, Hodoroaba V D, Langhoff N, Procop M, Rabe J and Wedell R 2005 *X-Ray Spectrom.* **34** 493

[3] Langer E, Dabritz S, Hauffe W and Haschke M 2005 *Appl. Surf. Sci.* **252** 240

[4] Lin X Y, Wang Z H, Sun T X, Pan Q L and Ding X L 2008 *Nucl. Instrum. Methods Phys. Res.* B **266** 2638

[5] Bjeoumikhov A, Langhoff N, Bjeoumikhova S and Wedell R 2005 *Rev. Sci. Instrum.* **76** 063115

[6] Yan Y M and Ding X L 2005 *X-Ray Spectrom.* **34** 235

[7] Liu A D 2005 *Nucl. Instrum. Methods Phys. Res.* B **234** 555

[8] Mildner D F R, Chen-Mayer H H and Gibson W M 2002 *J. Appl. Phys.* **92** 6911

[9] Matsuura Y, Oyama T and Miyagi M 2005 *Appl. Opt.* **44** 6193

[10] Mroczka R, Zukocinski R G and Kuczumow A 2005 *J. Alloys Compd.* **401** 108

[11] Mroczka R, Bartosik P, Sawłowicz Z, Skrzypiec K, Falkenberg G, Wójcik J, Żkociński G and Kuczumow A 2008 *Thin Solid Films* **516** 8029

[12] Singh S B, Poswal A K, Pandey M, Tokas R B, Chand N, Dhara S, Sundaravel B, Nair K G M, Sahoo N K and Patil D S 2009 *Surface and Coatings Technology* **203** 986

[13] Matyi R J, Depero L E, Bontempi E, Colombi P, Gibaud A, Jergel M, Krumrey M, Lafford T A, Lamperti A, Meduna M, van der Lee A and Wiemer C 2008 *Thin Solid Films* **516** 7962

[14] Edon V, Hugon M C, Agius B, Durand O, Eypert C and Cardinaud C 2008 *Thin Solid Films* **516** 7974